ACS Partner Journal

Journal of the American Society for Mass Spectrometry

pubs.acs.org/jasms

Research Article

Spontaneous Oxidation of Aromatic Sulfones to Sulfonic Acids in Microdroplets

Lingqi Qiu, Michael D. Psimos, and R. Graham Cooks*

Cite This: https://doi.org/10.1021/jasms.2c00029

Read Online

ACCESS | Metrics & More | Article Recommendations | Supporting Information

ABSTRACT: Reactions in microdroplets can be accelerated and can present unique chemistry compared to reactions in bulk solution. Here, we report the accelerated oxidation of aromatic sulfones to sulfonic acids in microdroplets under ambient conditions without the addition of acid, base, or catalyst. The experimental data suggest that the water radical cation, $(H_2O)^{+\bullet}$, derived from traces of water in the solvent, is the oxidant. The substrate scope of the reaction indicates the need for a strong electron-donating group (e.g., *p*-hydroxyl) in the aromatic ring. An analogous oxidation is observed in an aromatic ketone with benzoic acid production. The shared mechanism is suggested to involve field-assisted ionization of water at the droplet/air interface, its reaction with the sulfone (M) to form the radical cation adduct, $(M + H_2O)^{+\bullet}$, followed by 1,2-aryl migration and C−O cleavage. A remarkably high reaction rate acceleration ($\sim 10^3$) and regioselectivity (~100-fold) characterize the reaction.

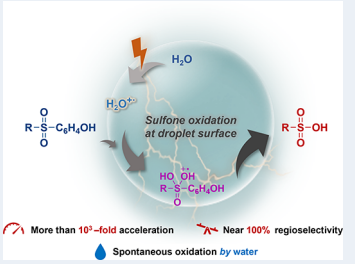

INTRODUCTION

Microdroplet chemistry has attracted much recent attention. The study of interfacial effects is facilitated by the large surface-to-volume ratio of microdroplets, which provide a platform for examination of chemistry at the surface. Chemical reactions in droplets are often accelerated compared to bulk solution,[1−9] and sometimes, they present unique reactivities. One good example is the occurrence of spontaneous oxidation (e.g., Dakin reaction of aldehydes to phenols) in aqueous microdroplets.[10] Zare and co-workers suggest that a strong electric field at the aqueous/air interface generates peroxy and hydroxyl radicals as the key reactive species.[11] Evidence for the strong fields at aqueous interfaces is available from spectroscopic studies[12] and is supported by computation.[13−15]

One-electron oxidation is a universal process associated with oxidative stress in biological systems.[16−18] Hydroxyl radicals play a key role, but other radical species may also contribute. One such species is the little-studied water radical cation, $(H_2O)^{+\bullet}$, which is present in pure bulk water[19] and can also be generated in quantity upon ionization of the vapor,[20] even under ambient conditions.[21] The radical cation/radical anion pair also exists fleetingly in pure bulk water. The radical cation undergoes fast proton transfer to generate the hydroxyl radical.[22,23] More significantly, the water radical cation is estimated to be the strongest oxidizing species in aqueous solutions,[24] with the standard redox potential of the $(H_2O)^{+\bullet}/H_2O$ couple (>3 V) being higher than that of $(HO\cdot + H^+)/H_2O$ (2.72 V).[23] This superior oxidative power should allow oxidization of compounds not oxidized by the hydroxyl radical.

Conventional bulk-phase oxidation of diaromatic sulfones to sulfonic acids, reported in a limited number of cases, requires either harsh conditions, such as strong bases with external promoters,[25] or well-designed metal catalysts.[26] Herein, we report the spontaneous oxidation of sulfones to sulfonic acids in microdroplets without external oxidants. Mechanistic studies suggest that the water radical cation, generated from the trace amounts of water in the organic solvent by the strong electric fields at the interface, is the key oxidant. An aromatic ketone is examined to explore the possibility that the reaction is more general in scope.

EXPERIMENTAL SECTION

All chemicals, including anhydrous magnesium sulfate and 4 Å molecular sieves, were purchased from Sigma-Aldrich (St. Louis, MO). Acetonitrile, methanol, and tetrahydrofuran were obtained from Fisher Scientific (Hampton, NH). Ethanol was acquired from Decon Laboratories (Sherman Oaks, CA). Information on prepared solutions not described in the main text is given in the Supporting Information (SI). The gas phase OH radical was generated by the Fenton reaction through mixing 30% H_2O_2 aqueous solution with 10 mM $FeCl_2$ aqueous solution (1:1) and confirmed using moisturized peroxide test strips from Merck KgaA (Darmstadt, Germany).

A Finnigan LTQ linear ion trap mass spectrometer (ThermoFisher Scientific, San Jose, CA) was used to perform nanoelectrospray ionization (nESI). The 10 μm internal diameter (I.D.) nanoelectrospray emitter was made using a micropipette tip puller to pull a borosilicate glass capillary (1.5

Special Issue: Focus: Gas-Phase Ion Chemistry

Received: January 29, 2022
Revised: March 10, 2022
Accepted: March 10, 2022

mm O.D.; 0.86 mm I.D.; 10 cm length). Both items were purchased from Sutter Instruments (Novato, CA). The spray voltage was +1.5 or −1.5 kV, depending on the chosen polarity, and the spray tip to inlet distance was 5 mm unless otherwise noted. Instrumental parameters were as follows: capillary temperature 150 °C; capillary voltage 15 V; tube lens 65 V. Note that for all comparison experiments, the samples were prepared in the same concentrations and solvents to correct for any product formation during nESI analysis.

RESULTS AND DISCUSSION

The negative ion mass spectrum (MS) of a methanol solution of 20 mM of 4,4′-sulfonylbis(2-methylphenol) (compound **1**) shows an unexpected peak at m/z 187 (Figure 1). This ion was

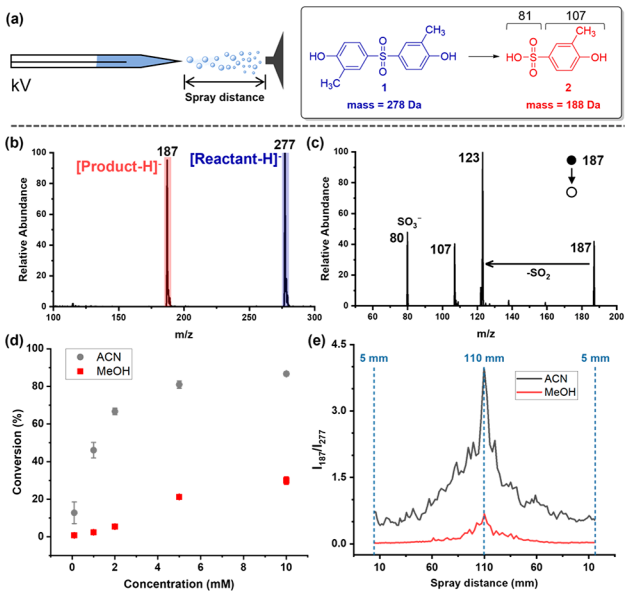

Figure 1. Oxidation of sulfone **1** in charged microdroplets generated by nESI. (a) Microdroplet oxidation of sulfone to sulfonic acid. (b) Mass spectrum in the negative mode, 20 mM sulfone **1** in methanol, at spray distance of 5 mm, showing only reactant and product. (c) MS/MS analysis of the generated sulfonic acid, m/z 187, showing characteristic fragments. (d) Reaction conversion, defined as ion intensity ratio $I_{187}/(I_{187} + I_{277})$, vs concentration in MeOH and ACN microdroplets. The error bars correspond to the standard deviation of three separate oxidation experiments using microdroplets. (e) Change in ion intensity ratio (I_{187}/I_{277}) for 1 mM sulfone **1** in ACN (upper trace) and MeOH (lower trace) as distance from sprayer to inlet is varied continuously from 5 to 110 mm and then back to 5 mm.

determined by MS/MS to be the deprotonated form of 4-hydroxy-3-methylbenzenesulfonic acid (**2**), as shown by the characteristic SO_2 and SO_3 losses and the formation of $SO_3^{-\bullet}$ (Figure 1c). Solutions of the sulfone were prepared in methanol and acetonitrile in concentrations that varied from 10 mM (the maximum concentration in acetonitrile) to 0.1 mM, and the results showed increased conversion of reactant to product with an increase in concentration (Figure 1d). This suggests the occurrence of oxidation of the sulfone (m/z 277) to the sulfonic acid (m/z 187). This reaction takes place in the microdroplets as indicated by the fact that the reaction in bulk (2 mL solution, 72 h) showed no product beyond the trace seen in freshly prepared solution (see Figure S1 in SI). The conversion factor, defined as the ion intensity ratio $I_{187}/(I_{187} + I_{277})$, was boosted when increasing the spray distance from 5 to 110 mm for both ACN and MeOH solutions (Figure 1d); the absolute intensities of product (m/z 187) decreased as expected (see Figure S2, SI) for spectra recorded at longer distance. The observed distance effect suggests that this transformation occurs in the charged microdroplets generated by nESI, with increased distances resulting in more evaporation and hence increased surface-to-volume ratios although the longer reaction times associated with droplet flight times will contribute also. The negligible conversion in bulk, less than 0.1%, indicates that the apparent acceleration factor, defined as the ratio of the conversion factor in microdroplets relative to that in bulk, is higher than 800. The much faster reaction rate, even without added reagents and under mild conditions, suggests that this unexpected reaction is driven by the unique chemistry of microdroplets.

The greater extent of reaction in acetonitrile vs methanol indicates a large solvent effect also seen for ethanol (EtOH) and tetrahydrofuran (THF), (see SI, Figure S3). More product was formed in more hygroscopic solvents,[27] such as ACN and EtOH, suggesting that absorbed water is important for the reaction. To test this assumption, we intentionally varied the amount of water in ACN, the best solvent. As expected, sulfone oxidation was prevented under completely anhydrous conditions (e.g., with the addition of water scavengers, such as molecular sieves and $MgSO_4$), although adding excess water (e.g., 1% H_2O in ACN) also hindered the reaction (Figure 2a). Similar trends were observed for another substrate, 4-(methylsulfonyl)phenol, with the greatest extent of reaction in this case being provided using 1% H_2O in ACN (see SI, Figure S4).

Significant additional evidence supporting the suggestion that water is involved in the oxidation is found in the positive ion mass spectrum of compound **1**. A unique peak at m/z 296 (Figure 2b) is assigned as $(M + H_2O)^{+\bullet}$. This species might be the protonated sulfone with an associated hydroxyl radical ($MH^+ \cdot HO$) or a complex of the sulfone and water radical cation $(M \cdot H_2O)^{+\bullet}$. It is notable that $(M + H_2O)^{+\bullet}$ was also observed in methanol droplets but with lower intensity (see SI, Figure S5), and this might be the reason for the lower conversion in methanol than in acetonitrile.

To explore the mechanism of sulfone oxidation in microdroplets, we added 30% H_2O_2 (aq.) to the solution to provide a 15% H_2O_2 (equivalent to 4.9 M) concentration, but this had no effect on the extent of product formation (SI, Figure S6a). The hydroxyl radical was also introduced in the gas phase, as illustrated in Figure S6b, and it too showed no effect, again suggesting that OH radicals/H_2O_2 are not the oxidant. To better understand the sulfone oxidation process, capture experiments were carried out. First, the radical trapping reagent TEMPO, (2,2,6,6-tetramethylpiperidin-1-yl)-oxyl, was added to the sulfone solution to interrupt the electron transfer process, and the product signal indeed dropped (SI, Figure S6c). Changing the gaseous environment from air to either ammonia vapor or formic acid vapor led to almost no product, presumably due to the consumption of the protonated species at the interface by the strong proton acceptor (ammonia) or the consumption of the oxidants by the electron acceptor (formic acid) (SI, Figure S6d).

From the above experimental evidence, we conclude that (i) a strongly oxidizing species is generated in those microdroplets, which contain trace amounts of water, so sulfone is converted to sulfonic acid; (ii) this species is present at the droplet surface and is deactivated in a gaseous environment

https://doi.org/10.1021/jasms.2c00029
J. Am. Soc. Mass Spectrom. XXXX, XXX, XXX−XXX

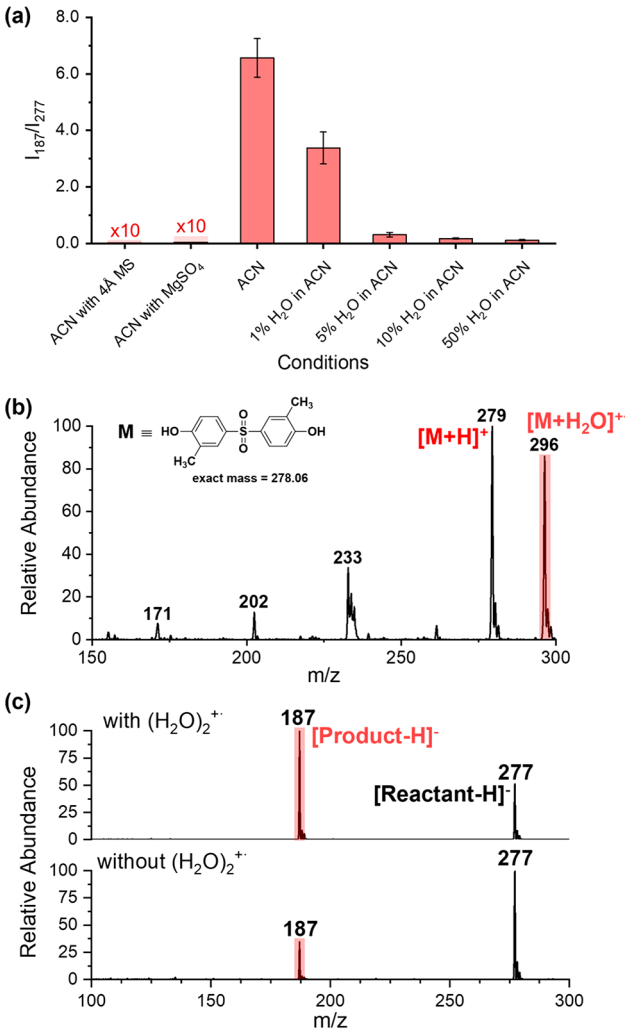

Figure 2. (a) Altering the amount of water in ACN dramatically changes the extent of the oxidation reaction. Removing all water prevents reaction. Optimum water concentration in ACN is <1%. (b) Mass spectrum in the positive mode. (c) Mass spectra of reaction mixtures with and without the addition of $(H_2O)_2^{+\bullet}$.

with a strong proton acceptor; (iii) this active species is a more powerful oxidant than OH radical/H_2O_2. As already noted, the water radical cation, $(H_2O)^{+\bullet}$, is a stronger oxidant than the OH radical. A recent study showed that the dimer of the water radical cation, $(H_2O)_2^{+\bullet}$, undergoes displacement reactions with a variety of analytes to form adducts,[28] which are formally analogous to the $(M + H_2O)^{+\bullet}$ adduct seen in Figure 2b. To test the concept that the water radical cation is the oxidant, $(H_2O)_2^{+\bullet}$ was produced using a home-built ambient corona discharge device operated at 1 kV. Figure S7 illustrates the apparatus and shows the mass spectrum of the generated water dimer radical cation.[28] This allowed deposition of the $(H_2O)_2^{+\bullet}$ spray (spray voltage 1 kV) onto the sulfone solution. To provide a negative control, the same protocol was followed but with 0 kV. As expected, the reaction with the addition of $(H_2O)_2^{+\bullet}$ gave a remarkably higher conversion to product than that without added $(H_2O)_2^{+\bullet}$ (see Figure 2c).

The reaction scope was explored using the optimized conditions, and product yields were measured as conversion factors calculated as the ion intensity of the product over the sum of product and reactant intensities (Table 1). Methyl substituents led to increased reaction, suggesting the

Table 1. Substrate Scope of Sulfone Oxidation[a]

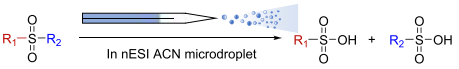

Entry	-R_1	-R_2	Product(s)	Conversion(s)[b]	Regio-selectivity[c]
1			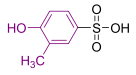	87%	N/A
2			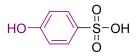	78%	N/A
3[d]			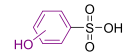	4%	N/A
4			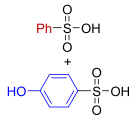	10% < 0.1%	>100:1
5			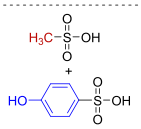	38% < 0.1%	>380:1
6			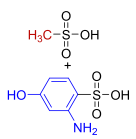	9% < 0.1%	>90:1
7			N/A	< 0.1%	N/A
8[e]		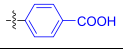	N/A	< 0.1%	N/A

[a]Reactions were performed at 10 mM concentration in ultrahigh-purity acetonitrile, which was not especially dried. [b]Conversion (measure of product yield) was calculated as ion intensity of product over the sum of product and reactant intensities. [c]Regioselectivity was calculated as the conversion of R_1SO_3H relative to that of R_2SO_3H. [d]These two products share the same m/z and so are not distinguished. [e]A 2 mM concentration was used for benzoate due to its moderate solubility in acetonitrile.

importance of electron donation in the aryl ring as indicated by the *p*-hydroxyl (entry 2). Moving the hydroxyl group from the *para*- to *ortho*-position caused a large decrease in conversion to product, presumably due to the steric hindrance at the reaction site (entry 3). Asymmetric sulfones with different R_1 groups were also investigated (entries 4 and 5). The fact that a single product was seen in every case indicates the very high regioselectivity in the sulfone oxidation. The fact that no conversion was observed for the sulfone with a *p*-carboxylic acid group (entry 8) again demonstrates the significance of R_2 being strongly electron-donating. Other changes were made to the R_2 group, including adding an amino or a fluoro substituent; both decreased the yield, presumably due to the high proton affinity and the strong electron-withdrawing effects, respectively.

The generation of the water radical cation can occur in two ways: (i) Water is ionized by the strong electric field at or near the aqueous droplet surface, generating the water radical cation; (ii) charge transfer produces water radical cations/radical anions even in bulk water from hydrogen-bonded water molecules.[19,29] Given that the presence of water and a high potential are both involved in the successful oxidations studied here, we suggest that the strong electric field is responsible for

https://doi.org/10.1021/jasms.2c00029
J. Am. Soc. Mass Spectrom. XXXX, XXX, XXX−XXX

the generation of the water radical cation. These ions react with the sulfone to generate the sulfonic acid via adduct formation, which is expected to be highly favorable at the microdroplet interface. More than 1% water may facilitate conversion to hydronium and the hydroxyl radical, thus leading to the lower reaction. Note further that the generated water radical cations may exist as the dimer, $[H_2O\cdots OH_2]^{+\bullet}$, a species known to exist as the O−O weakly bonded dimer.[30] The dimer could undergo a displacement reaction[28] with the sulfone to produce a radical cation adduct **A**, or this species might be formed by direct addition to the monomeric water radical cation (Scheme 1). Adduct formation is suggested to be

Scheme 1. Proposed Mechanism of Sulfone Oxidation in Microdroplets

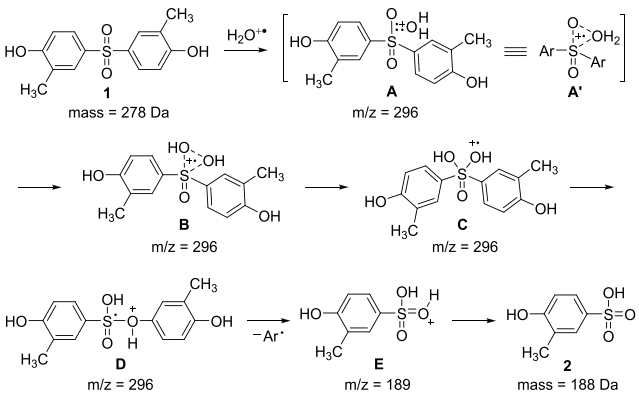

followed by proton transfer to form a geminal diol structure (**C**). 1,2-Aryl migration then generates the sulfinic acid **D**. The migration is expected to follow the order −Ph−OH > −Ph > −alkyl,[31,32] explaining the high regioselectivity observed in Table 1, entries 4−6. Partial solvation of interfacial species at the droplet surface might contribute to the ∼10^3-fold reaction acceleration in microdroplets, and this acceleration will also amplify the regioselectivity. The high reactivity of aryl sulfonate (similar to aryl halide) and the relatively low bond dissociation energy of phenolic Csp^2−OH (86 kcal/mol),[33] may facilitate the elimination of an aryl radical and thus provide the protonated sulfonic acid **E**. Final deprotonation would give the corresponding sulfonic acid **2** as the product, although the phase in which the last two steps occur is not elucidated.

The reaction between sulfone and the water radical cation, especially the formation of the geminal diol intermediate in the proposed mechanism, triggered our interest in the possible analogous oxidation of aromatic ketones. Some pioneering studies on water radical cation chemistry examined its reaction with carbonyl compounds, e.g., acetone[34] and ethyl acetate,[28] and in both of these cases, the radical cation complex, $(M + H_2O)^{+\bullet}$, was observed. However, no corresponding oxidation products were reported. Since the phenolic hydroxyl group on the aryl ring is seen to drive 1,2-migration, 4-hydroxybenzophenone was chosen as the substrate in this new study. In both methanol and acetonitrile, $(M + H_2O)^{+\bullet}$, m/z 216, was observed (Figure 3a and SI, Figure S8); weak binding is indicated by the fact that it was lost during in-source fragmentation (SI, Figure S9). In the negative mode, the carboxylic acid product was observed in methanol droplets (Figure 3b), as confirmed by MS/MS (SI, Figure S10). The occurrence of a single product verified the high regioselectivity

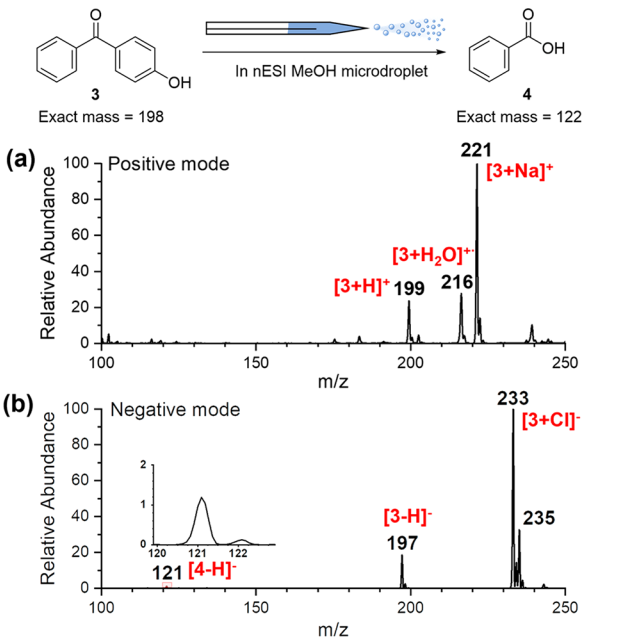

Figure 3. Oxidation of 4-hydroxybenzophenone in charged microdroplets generated by nESI. (a) Mass spectrum in the positive mode, showing $(M + H_2O)^{+\bullet}$ at m/z 216. (b) Mass spectrum in the negative mode, where reactant **3** and product **4** were both observed.

in the ketone as in the sulfone oxidation. These results suggest that the ketone oxidation shares a similar mechanism (SI, Figure S11) to the sulfone oxidation.

CONCLUSION

In summary, we report the spontaneous oxidation of sulfones to sulfonic acids in microdroplets without external oxidants. The reaction occurs at the droplet interface and is accelerated by a large factor over oxidation in bulk solution. The reaction is explored in terms of effects of solvent composition, substrate nature and concentration, and droplet flight distance as well as in a polarity reversal experiment where the water radical cation adducts were observed. The data demonstrate the importance of traces of water in the organic solvent. However, adding H_2O_2 and/or hydroxyl radical in either the solution phase or the droplet phase did not increase product formation, suggesting that hydroxyl radicals are not the reactive species. By contrast, adding an external water dimer radical cation into the reaction solution increases reactant to product conversion. These facts indicate that the water radical cation, presumably formed at the droplet surface by the high electric field, is the oxidant. The proposed mechanism involves radical cation adduct formation, 1,2-aryl migration, and C−O cleavage. It is consistent with the substrate scope finding that a strongly electron-donating hydroxyl group in the *para*-position of the aromatic sulfone is needed. The magnitude of the regioselectivity is extraordinarily large, consistent with the observed acceleration of the reaction. An analogous transformation was observed in an aromatic ketone, suggesting the generality of water radical cation oxidation and its likely applicability to P═O, P═S, and C═N systems.

ASSOCIATED CONTENT

Supporting Information

The Supporting Information is available free of charge at https://pubs.acs.org/doi/10.1021/jasms.2c00029.

https://doi.org/10.1021/jasms.2c00029
J. Am. Soc. Mass Spectrom. XXXX, XXX, XXX−XXX

Additional experimental details and materials, including mass spectrum and illustration of experimental setup (PDF)

AUTHOR INFORMATION

Corresponding Author

R. Graham Cooks − *Department of Chemistry, Purdue University, West Lafayette, Indiana 47907, United States;* orcid.org/0000-0002-9581-9603; Email: cooks@purdue.edu

Authors

Lingqi Qiu − *Department of Chemistry, Purdue University, West Lafayette, Indiana 47907, United States*

Michael D. Psimos − *Department of Chemistry, Purdue University, West Lafayette, Indiana 47907, United States*

Complete contact information is available at: https://pubs.acs.org/10.1021/jasms.2c00029

Author Contributions

R.G. Cooks and L. Qiu designed the experiments. L. Qiu and M. D. Psimos performed the experiments. The manuscript was written through contributions of all authors.

Notes

The authors declare no competing financial interest.

ACKNOWLEDGMENTS

The authors acknowledge financial support from the National Science Foundation (Grant number CHE-1905087) and from the Multidisciplinary University Research Iniative (MURI) Program of the Air Force Office of Scientific Research (FA9550-21-1-0170) via Stanford University (subaward 62741613-204669).

DEDICATION

Dedicated to Peter Armentrout in celebration of the quantity and quality of his contributions to ion chemistry.

REFERENCES

(1) Yan, X.; Bain, R. M.; Cooks, R. G. Organic Reactions in Microdroplets: Reaction Acceleration Revealed by Mass Spectrometry. *Angew. Chemie Int. Ed.* **2016**, *55* (42), 12960−12972.

(2) Wei, Z.; Li, Y.; Cooks, R. G.; Yan, X. Accelerated Reaction Kinetics in Microdroplets: Overview and Recent Developments. *Annu. Rev. Phys. Chem.* **2020**, *71* (1), 31−51.

(3) Cooks, R. G.; Yan, X. Mass Spectrometry for Synthesis and Analysis. *Annu. Rev. Anal. Chem.* **2018**, *11* (1), 1−28.

(4) Müller, T.; Badu-Tawiah, A.; Cooks, R. G. Accelerated Carbon-Carbon Bond-Forming Reactions in Preparative Electrospray. *Angew. Chemie - Int. Ed.* **2012**, *51* (47), 11832−11835.

(5) Crawford, E. A.; Esen, C.; Volmer, D. A. Real Time Monitoring of Containerless Microreactions in Acoustically Levitated Droplets via Ambient Ionization Mass Spectrometry. *Anal. Chem.* **2016**, *88* (17), 8396−8403.

(6) Vannoy, K. J.; Lee, I.; Sode, K.; Dick, J. E. Electrochemical Quantification of Accelerated FADGDH Rates in Aqueous Nanodroplets. *Proc. Natl. Acad. Sci. U. S. A.* **2021**, *118* (25), e2025726118.

(7) Sahota, N.; AbuSalim, D. I.; Wang, M. L.; Brown, C. J.; Zhang, Z.; El-Baba, T. J.; Cook, S. P.; Clemmer, D. E. A Microdroplet-Accelerated Biginelli Reaction: Mechanisms and Separation of Isomers Using IMS-MS. *Chem. Sci.* **2019**, *10* (18), 4822−4827.

(8) Zhong, X.; Chen, H.; Zare, R. N. Ultrafast Enzymatic Digestion of Proteins by Microdroplet Mass Spectrometry. *Nat. Commun.* **2020**, *11* (1), 1049.

(9) Zhang, W.; Zheng, B.; Jin, X.; Cheng, H.; Liu, J. Rapid Epoxidation of α,β-Unsaturated Olefin in Microdroplets without Any Catalysts. *ACS Sustain. Chem. Eng.* **2019**, *7* (17), 14389−14393.

(10) Gao, D.; Jin, F.; Lee, J. K.; Zare, R. N. Aqueous Microdroplets Containing Only Ketones or Aldehydes Undergo Dakin and Baeyer-Villiger Reactions. *Chem. Sci.* **2019**, *10* (48), 10974−10978.

(11) Chamberlayne, C. F.; Zare, R. N. Simple Model for the Electric Field and Spatial Distribution of Ions in a Microdroplet. *J. Chem. Phys.* **2020**, *152* (18), 184702.

(12) Xiong, H.; Lee, J. K.; Zare, R. N.; Min, W. Strong Electric Field Observed at the Interface of Aqueous Microdroplets. *J. Phys. Chem. Lett.* **2020**, *11* (17), 7423−7428.

(13) Leung, K. Surface Potential at the Air−Water Interface Computed Using Density Functional Theory. *J. Phys. Chem. Lett.* **2010**, *1* (2), 496−499.

(14) Cendagorta, J. R.; Ichiye, T. The Surface Potential of the Water−Vapor Interface from Classical Simulations. *J. Phys. Chem. B* **2015**, *119* (29), 9114−9122.

(15) Hao, H.; Leven, I.; Head-Gordon, T. Can Electric Fields Drive Chemistry for an Aqueous Microdroplet? *Nat. Commun.* **2022**, *13* (1), 280.

(16) Imlay, J. A.; Linn, S. DNA Damage and Oxygen Radical Toxicity. *Science (80-.)* **1988**, *240* (4857), 1302−1309.

(17) Cadet, J.; Douki, T.; Ravanat, J.-L. One-Electron Oxidation of DNA and Inflammation Processes. *Nat. Chem. Biol.* **2006**, *2* (7), 348−349.

(18) Pizzino, G.; Irrera, N.; Cucinotta, M.; Pallio, G.; Mannino, F.; Arcoraci, V.; Squadrito, F.; Altavilla, D.; Bitto, A. Oxidative Stress: Harms and Benefits for Human Health. *Oxid. Med. Cell. Longev.* **2017**, *2017*, 1−13.

(19) Lee, A. J.; Rick, S. W. The Effects of Charge Transfer on the Properties of Liquid Water. *J. Chem. Phys.* **2011**, *134* (18), 184507.

(20) Karpas, Z.; Huntress, W. T. Reactions of OH+ and H2O+ Ions with Some Diatomic and Simple Polyatomic Molecules. *Chem. Phys. Lett.* **1978**, *59* (1), 87−89.

(21) Chingin, K.; Liang, J.; Hang, Y.; Hu, L.; Chen, H. Rapid Recognition of Bacteremia in Humans Using Atmospheric Pressure Chemical Ionization Mass Spectrometry of Volatiles Emitted by Blood Cultures. *RSC Adv.* **2015**, *5* (18), 13952−13957.

(22) Gauduel, Y.; Pommeret, S.; Migus, A.; Antonetti, A. Some Evidence of Ultrafast H2O+-Water Molecule Reaction in Femtosecond Photoionization of Pure Liquid Water: Influence on Geminate Pair Recombination Dynamics. *Chem. Phys.* **1990**, *149* (1−2), 1−10.

(23) Ma, J.; Wang, F.; Mostafavi, M. Ultrafast Chemistry of Water Radical Cation, H2O●+, in Aqueous Solutions. *Molecules* **2018**, *23* (2), 244.

(24) Ma, J.; Schmidhammer, U.; Pernot, P.; Mostafavi, M. Reactivity of the Strongest Oxidizing Species in Aqueous Solutions: The Short-Lived Radical Cation H2O●+. *J. Phys. Chem. Lett.* **2014**, *5* (1), 258−261.

(25) Yang, H.; Chu, D.-Z.; Jiao, L. Aromatization Modulates the Activity of Small Organic Molecules as Promoters for Carbon−Halogen Bond Activation. *Chem. Sci.* **2018**, *9* (6), 1534−1539.

(26) Srimani, D.; Leitus, G.; Ben-David, Y.; Milstein, D. Direct Catalytic Olefination of Alcohols with Sulfones. *Angew. Chemie Int. Ed.* **2014**, *53* (41), 11092−11095.

(27) Tan, B.; Melius, P.; Ziegler, P. A Simple Gas Chromatographic Method for the Study of Organic Solvents: Moisture Analysis, Hygroscopicity, and Evaporation. *J. Chromatogr. Sci.* **1982**, *20* (5), 213−217.

(28) Wang, M.; Gao, X.-F.; Su, R.; He, P.; Cheng, Y.-Y.; Li, K.; Mi, D.; Zhang, X.; Zhang, X.; Chen, H.; Cooks, R. G. Abundant Production of Reactive Water Radical Cations under Ambient Conditions. *CCS Chem.* **2021**, 3559−3566.

(29) Ben-Amotz, D. Unveiling Electron Promiscuity. *J. Phys. Chem. Lett.* **2011**, *2* (10), 1216−1222.

(30) Cheng, Q.; Evangelista, F. A.; Simmonett, A. C.; Yamaguchi, Y.; Schaefer, H. F. Water Dimer Radical Cation: Structures, Vibrational

Frequencies, and Energetics. *J. Phys. Chem. A* **2009**, *113* (49), 13779−13789.
(31) Aureliano Antunes, C. S.; Bietti, M.; Ercolani, G.; Lanzalunga, O.; Salamone, M. The Effect of Ring Substitution on the O -Neophyl Rearrangement of 1,1-Diarylalkoxyl Radicals. A Product and Time-Resolved Kinetic Study. *J. Org. Chem.* **2005**, *70* (10), 3884−3891.
(32) Marx, J. N.; Argyle, J. C.; Norman, L. R. Migration of Electronegative Substituents. I. Relative Migratory Aptitude and Migration Tendency of the Carbethoxy Group in the Dienone-Phenol Rearrangement. *J. Am. Chem. Soc.* **1974**, *96* (7), 2121−2129.
(33) Qiu, Z.; Li, C.-J. Transformations of Less-Activated Phenols and Phenol Derivatives via C−O Cleavage. *Chem. Rev.* **2020**, *120* (18), 10454−10515.
(34) Zhang, X.; Ren, X.; Zhong, Y.; Chingin, K.; Chen, H. Rapid and Sensitive Detection of Acetone in Exhaled Breath through the Ambient Reaction with Water Radical Cations. *Analyst* **2021**, *146* (16), 5037−5044.

https://doi.org/10.1021/jasms.2c00029
J. Am. Soc. Mass Spectrom. XXXX, XXX, XXX−XXX